

# Experiments of ultrasonically aided micro-EDM on Ti with nanostructured superficial TiO<sub>2</sub> layers

Niculae Marinescu<sup>1</sup>, Daniel Ghiculescu<sup>1,\*</sup>, Stergios Ganatsios<sup>2</sup> and George Seritan<sup>3</sup>

<sup>1</sup> “Politehnica” University of Bucharest, Department of Manufacturing Engineering, 313 Splaiul Independentei, sector 6, Bucharest, Romania

<sup>2</sup> Technological Educational Institute of Western Macedonia, Department of Electrical Engineering, GR50100 Kila Kozani, Greece.

<sup>3</sup> “Politehnica” University of Bucharest, Department of Measurements, Electrical Devices and Static Converters, 313 Splaiul Independentei, sector 6, Bucharest, Romania

**Abstract.** The paper deals with experimental researches concerning micro-machining through ultrasonically aided electrical discharge machining ( $\mu$ EDM+US) of an advanced material, comprising a base metal from Ti and superficial nanometric layers from TiO<sub>2</sub>, i.e. Titania nanotube arrays. The material was investigated by scanning electron microscope. The chemical composition of machined samples was determined by X rays spectrometer energy dispersive. The roughness of machined surface was studied using a profile surface instrument. A comparison was made between the results obtained by classic  $\mu$ EDM and  $\mu$ EDM+US in terms of surface roughness, and craters microgeometry.

## 1 Introduction

Titania nanotube arrays anodically grown represent an advanced and interesting material from the point of view of large range of applications [1]. Some illustrative examples with its particular requirements are: photocatalysis through water splitting and simultaneous organic pollutant decomposition, providing uniform electric field distribution for effective charges transfer, as well as superior capabilities of light harvesting [2], gas sensing - highly sensitive to hydrogen [3], energy conversion at fabrication of dye-sensitized solar cells [4], energy storage at production of electrostatic capacitors based on super dielectric material (titania nanotubes filled with concentrated aqueous salt solutions) [5], and biomedicine due to protection of the surface from corrosion, prevention of ion release and osseointegration of these biomaterials [6].

High hardness of titanium dioxide that can attain 16.1 GPa in case of rutile deposited by modulated plasma, and 4.8 GPa at anatase obtained conventionally by magnetron sputtering [7]. Both thin coated films of under micron thickness are considered as scratch resistant, proving high wear resistance in different mechanical applications. But this level of mechanical properties determines consistent difficulties at conventional machining. Therefore nonconventional machining, nonrelated to mechanical properties, but to thermal

---

\* Corresponding author and co-author(s): [daniel.ghiculescu@upb.ro](mailto:daniel.ghiculescu@upb.ro)

ones, like micro-electrical discharge machining ( $\mu$ EDM) represent nowadays solutions in the domain of micro and even nano-size [8]. Moreover ultrasonically aided electrical discharge machining ( $\mu$ EDM+US) could be a recent competitive response of all these, in terms of machining rate, precision and surface quality in relation with manufacturing costs [9]. Other advanced materials, difficult to process with other means, were machined by  $\mu$ EDM+US with spectacular increase of main technological performances [10].

## 2 Experimental setup

An experimental setup (Figure 1), installed on Romanian ELER 01 machine, was created to study the micro-EDM+US process on nanostructured material (samples of 30 x 30 x 1 mm) formed by a superficial layer from Titania nanotube arrays grown on Ti base. The machining tests were performed with 20 kHz longitudinal ultrasonic oscillations of tool-electrode (EDM+US), and without US (classic EDM). A device for clamping the ultrasonic chain, included the tool at its end - a granted patent [11] - was used.

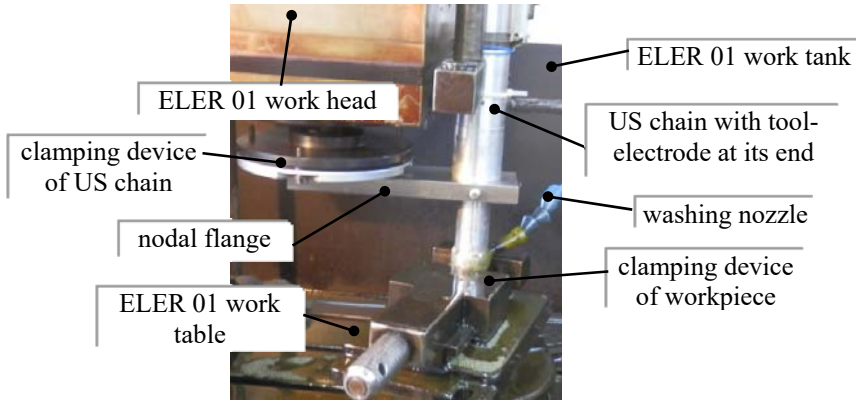


**Fig. 1.** Technological system for microEDM+US of Titania nanotube arrays on Ti base.

Both commanded and relaxation pulses were used, provided by a special generator dedicated to finishing and micro-machining, connected to ELER 01 machine. The working parameters were: at commanded pulses, current step,  $I=3$  A, positive (tool) polarity, lateral flushing with pressure,  $p_{ht}=0.04$  MPa, pulse time  $t_i=48$   $\mu$ s, pause time,  $t_0=24$   $\mu$ s - *working mode no. 1*;  $t_i=95$   $\mu$ s,  $t_0=24$   $\mu$ s - *working mode no. 2*; at relaxation pulses, negative polarity, capacitor step,  $C=10$  nF, resistance step,  $R=0.74$  k $\Omega$  (for adjusting supply current) - *working mode no. 3*. At  $\mu$ EDM+US, the consumed power on ultrasonic chain ( $P_{cUS}$ ) was 80, 90 W.

The total hydraulic pressure ( $p_{ht}$ ) in the gap varies in phase with elongation ( $z$ ), according to relation:

$$p_{ht} = 2\pi c \rho f_{US} z + p_{ht} \text{ [Pa]}, \quad (1)$$

where:  $c$  is sound velocity in dielectric liquid [m/s];  $\rho$  - dielectric liquid density [kg/m<sup>3</sup>];  $f_{US}$  - ultrasonic frequency [Hz];  $z$  - elongation,  $z=Asin \omega t$ ;  $A$  - amplitude [m];  $\omega = 2\pi f_{US}$  [s<sup>-1</sup>];  $p_{ht}$  - local hydraulic pressure [Pa]. In this case, the values of parameters were:  $p_{ht}=0.04$  MPa,  $\rho=840$  kg/m<sup>3</sup> (P3 dielectric liquid with kinematic viscosity, 3 m<sup>2</sup>/s),  $K=1.35 \times 10^9$  Pa ( $K$ -bulk modulus),  $c=(K/\rho)^{1/2}=1267.7$  m/s,  $A=2$   $\mu$ m,  $f_{US}=20$  kHz.

At each final of ultrasonic period  $T_{US}$ , the *cumulative microjets stage* (CMS) is produced by collective implosion of gas bubbles from the gap. Thus, pressure, of 100 MPa order is generated, by shock waves, oriented along the frontal gap.

### 3 Analysis of chemical composition and microtopography

The X rays spectrometer energy dispersive (EDS) with resolution at MnK of 133 eV was used to determine the chemical composition of samples to be machined, i.e. approximately (slight variation at different analyzed samples) 25 weight % for O, and 75 % for Ti. So, three working modes, EDM and EDM+US, were comparatively applied on all samples.

Investigation of machined samples microtopography was made by scanning electron microscope QUANTA INSPECT F50, provided with field emission electron gun with resolution of 1 nm. Firstly, the superficial layer of Titania nanotubes anodically grown on Ti base was studied, determining the lengths under 600 nm, diameters of 54... 95 nm, and walls thickness of 11... 15 nm, resulted from images like those presented in Figure 1.

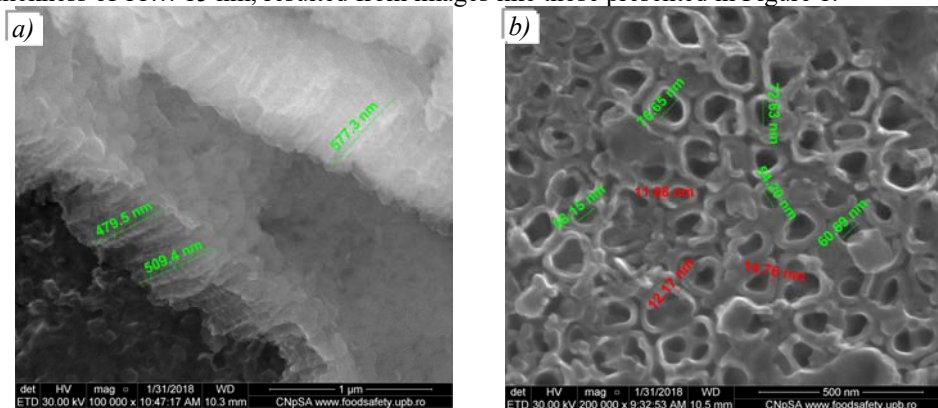


**Fig. 2.** Dimensions of anodically grown Titania nanotubes (a) lateral view; (b) frontal view.

Despite the electric isolator character of  $\text{TiO}_2$ , the micro-electrical discharge machining was possible due to very small thickness of nonconductive superficial layer on Ti base.

The images of machined microtopography obtained at pure  $\mu\text{EDM}$  with working mode no.1 are presented in Figure 2.a for a central zone located within the machining mark. The machined surface roughness was  $R_z=4 \mu\text{m}$ , determined by SJ411 surface instrument. The average of craters transversal dimensions was  $D_{cr}=10 \mu\text{m}$ . Many of craters are overlapped due to several discharges produced in the very proximity. In this case, it is considered that depth of machining is deeper than the superficial layer of Titania.

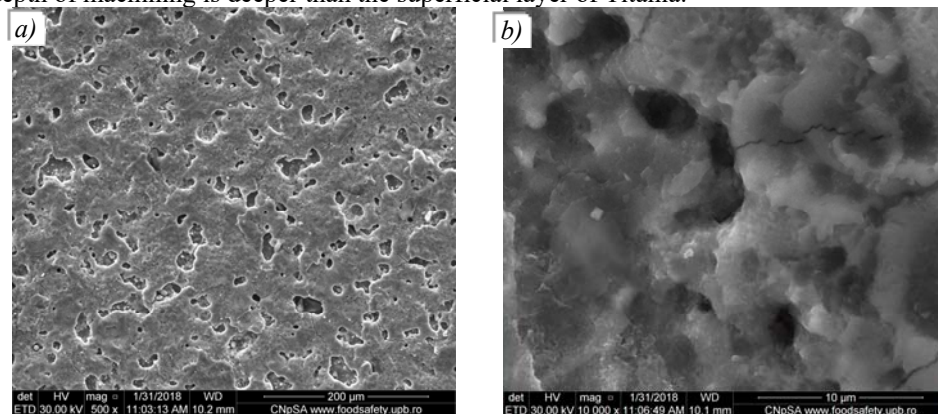


**Fig. 3.** Microtopography at EDM,  $I=3\text{A}$ ,  $t_i=48 \mu\text{s}$ ,  $t_o=24 \mu\text{s}$ , polarity +; (a) middle; (b) margin.

Another image was taken from a marginal zone (Figure 2.b) with only first several craters produced by starting discharges, considered to be located on the superficial layer of Titania. In this case, the average of craters diameters is  $D_{cr}=2 \mu\text{m}$ .

At  $\mu\text{EDM}+\text{US}$  with working mode no.1, with consumed power on US chain,  $P_{CUS} = 90 \text{ W}$ , the resulted images of machined microtopography from the mark interior obtained with this working mode, are presented in Figure 3.a. In this case, the sample roughness was  $Rz=2.8 \mu\text{m}$ , and the average of craters transversal dimensions was  $D_{cr}=6 \mu\text{m}$ . As it can be noticed, a decrease of crater volume is produced due to ultrasonic assistance not only in terms of diameter but also in depth, which is related to  $Rz$ . A specific phenomena also occurred: a large amount of molten material and resolidified covers the machined surface, which in addition presents some microcracks of under  $1 \mu\text{m}$  width, which creates difficulty in identification of craters resulted from single discharges.

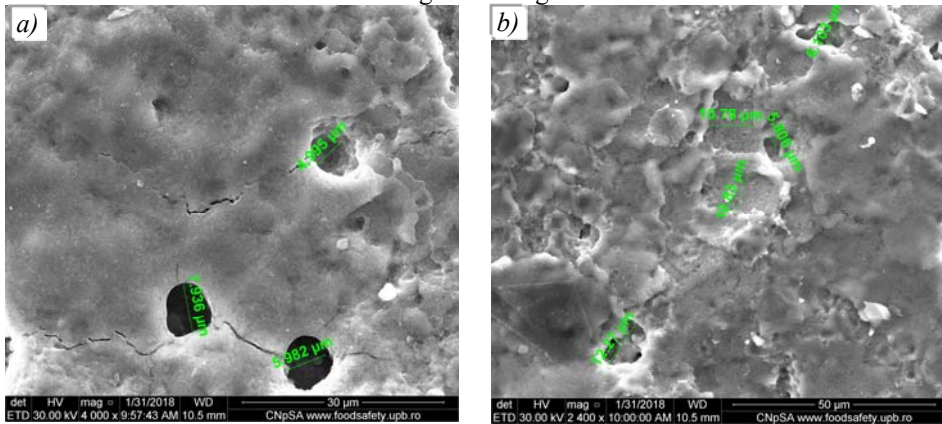


**Fig. 4.** Microtopography at  $\mu\text{EDM}+\text{US}$ ,  $I=3\text{A}$ ,  $t=48 \mu\text{s}$ ,  $t_0=24 \mu\text{s}$ , polarity +;  $P_{CUS} = 90 \text{ W}$ ; (a) middle; (b) margin.

This results could be the effect of CMS. During EDM+US process, the pulses are delivered within  $T_{US}$ . When pulse duration is overlapped on CMS, it was noticed experimentally that EDM discharge is stopped [8]. Since the gas bubble formed around plasma channel collapses due to CMS, the dielectric liquid enters the zone of discharge spot, and removes the workpiece material still in liquid phase. Moreover, the shock waves cut the margins of the craters, determining the roughness decrease as well as crater diameters. As before, images were taken from the margins of the machined mark, like this presented in Figure 3.b. No significant difference in terms of average crater diameters was obtained, but the surface is covered with lower amount of molten material and resolidified. This pointed out that ultrasonic assistance is able to rapid penetration of Titania of superficial layer, the craters being formed already inside the Ti base, like in the Figure 3.a.

The images obtained at classic  $\mu\text{EDM}$  with working mode no. 2 are presented in Figure 4. The sample roughness was  $Rz=6 \mu\text{m}$ , and the average of craters transversal dimensions was  $D_{cr}=15 \mu\text{m}$  in the interior of the mark obtained at this working mode. It can be noticed almost the same aspect as at previous working mode with many overlapped craters and much resolidified material, covering the machined surface (Figure 2.a). At the margin of the mark, the crater diameters were much smaller with mean diameter  $D_{cr}=2.2 \mu\text{m}$ , larger than at previous working mode, the pulse duration being longer. As it can be noticed, it is confirmed thus, that classic  $\mu\text{EDM}$  has lower capacity to penetrate the superficial layer of Titania nanotubes by first discharges, producing smaller craters than in the middle of the machined mark.

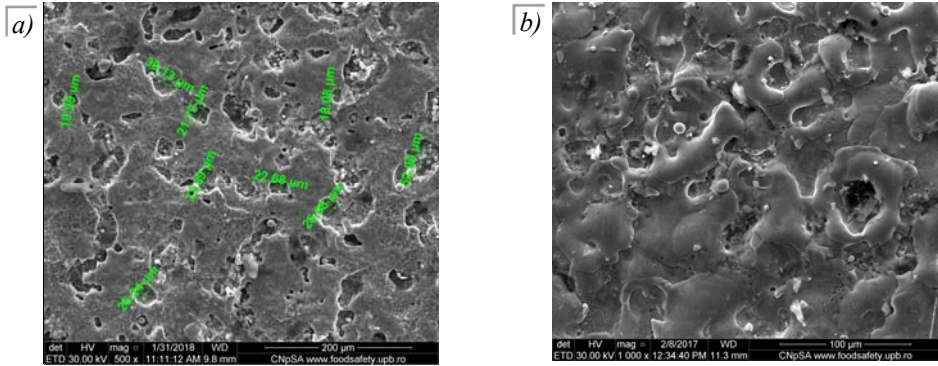


**Fig. 5.** Microtopography at  $\mu$ EDM,  $I=3A$ ,  $t_f=95 \mu s$ ,  $t_0=24 \mu s$ , polarity +; (a) middle; (b) margin.

At  $\mu$ EDM+US and the same working mode, no. 2, with power consumed on the US chain,  $P_{CUS} = 90 W$ , the microtopography is shown in Figure 5. Average craters diameters in the middle was  $D_{cr}=12 \mu m$  (Figure 5.a), and about the same at the margin (Figure 5.b), based on the former described phenomena. The machined surface roughness was  $R_z=5.2 \mu m$ . Nevertheless, longer pulse time  $t_f=95 \mu s$  with high probability of overlapping on CMS produces larger craters in terms of diameter and depth than at previous working mode.

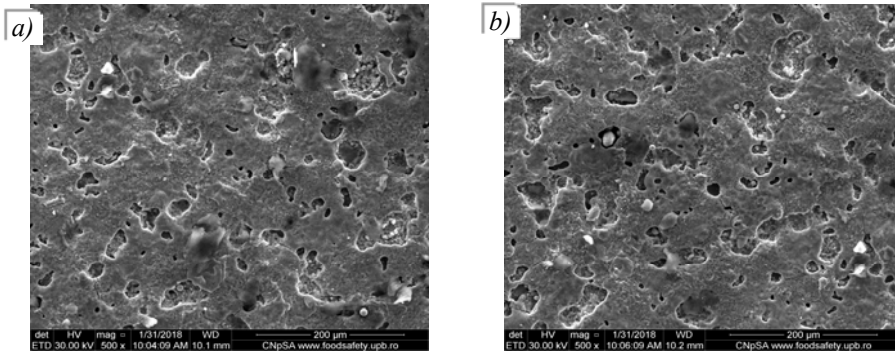


**Fig. 6.** Microtopography at  $\mu$ EDM,  $I=3A$ ,  $t_f=95 \mu s$ ,  $t_0=24 \mu s$ , polarity +;  $P_{CUS} = 90 W$ ; (a) middle; (b) margin.

At  $\mu$ EDM with relaxation pulses, working mode no. 3, the resulted microtopography is presented in Figure 6. The sample roughness was  $R_z=2\mu m$ , the average of craters transversal dimensions was  $D_{cr}=13 \mu m$ , flatter craters, specific to relaxation pulses.

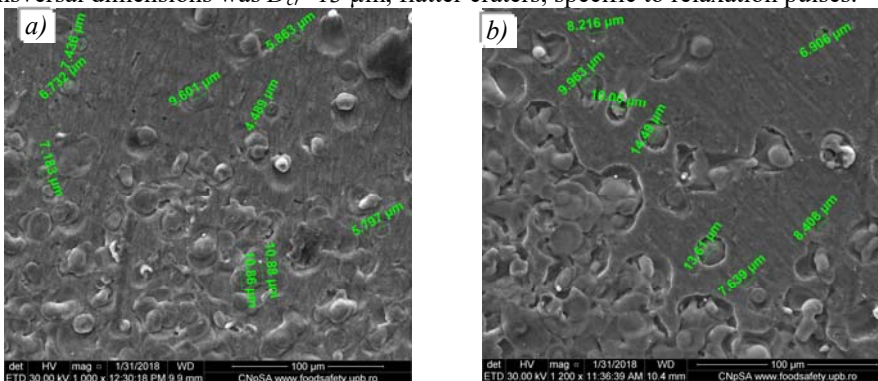


**Fig. 7.** Microtopography at  $\mu$ EDM,  $C=10 nF$ ,  $R=0.74 k\Omega$ , polarity -; (a) middle; (b) margin.

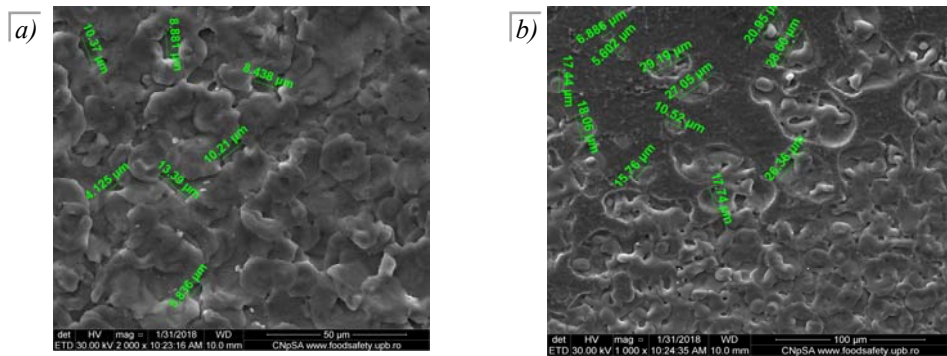


**Fig. 8.** Microtopography at  $\mu$ EDM+US,  $C=10$  nF,  $R=0.74$  k $\Omega$ , polarity - ;  $P_{CUS} = 70$  W; (a) middle; (b) margin.

At  $\mu$ EDM+US with relaxation pulses, working mode no. 3, with lower power,  $P_{CUS} = 70$  W - appropriate to relaxation craters shape [8] - the images of microtopography are presented in Figure 7. The diametric variation is larger than in previous cases due to specific lack of control of pulse duration. In this last case, the roughness was  $R_z=1.6$   $\mu$ m, and the average of craters transversal dimensions was  $D_{cr}=10$   $\mu$ m. The craters diameters varies in almost the same range in case of images taken from the middle or the margin of machined mark.

## 4 Conclusions

The advanced material, comprising a Ti base and a thin layer of TiO<sub>2</sub> nanotubes anodically grown, is difficult to micromachine by classic cutting due to its high hardness. Ultrasonic assistance enhance the capacity of microEDM to penetrate the isolator superficial layer of TiO<sub>2</sub>. The use of commanded pulses with relative long duration determines the increase of machining rate because of the high probability to overlap the pulse duration on cumulative microjets stage, which allows the dielectric liquid to remove a high amount of melted material. The use of relaxation pulses is superior in terms of surface roughness due to flatter craters in comparison to those obtained with commanded pulses. In both cases, the reduced power on ultrasonic chain can remove the margin of the craters, leading to decrease the crater diameters and their depth, thus improving the surface roughness.

The SEM analyzes/images obtained on the samples were possible due to EU-funding project POSCCE-A2-O2.2.1-2013-1/Priority Axe 2, Project No. 638/12.03.2014, ID 1970, SMIS-CSNR code 48652.

## References

1. F.J.Q. Cortes et al., *Materials & Design* **96**, 80-89 (2016)
2. H. Wu, Z. Zhang, *J. Solid State Chemistry* **184**, 12, 3202-3207 (2011)
3. O.K. Varghese et al., *Sensors and Actuators B: Chemical* **93**, 1-3, 338-344 (2003)
4. H. Park, *Solar Energy Materials and Solar Cells* **95**, 1, 184-189 (2011)
5. F.J.Q. Cortes, J. Phillips, *Materials* **8**, 6208-6227 (2015)
6. S. Minagar, *Acta biomaterialia* **8**, 2875-2888 (2012)
7. D. Wojcieszak et al., *Materials Science-Poland* **33**, 660-668 (2015)
8. M. P. Jahan, et al., *Electrical Discharge Machining (EDM)*. (Nova, New York, 2015)
9. P. Singh et al., *Int. J. Adv. Manuf. Technol.* **94**, 2551-2562 (2017)
10. H. Ni et al., *Int. J. Adv. Manuf. Technol.* **93**, 1-8 (2018)
11. D. Ghiculescu, N.I. Marinescu, S. Nanu, Romanian granted patent, RO-126191 (2012)